



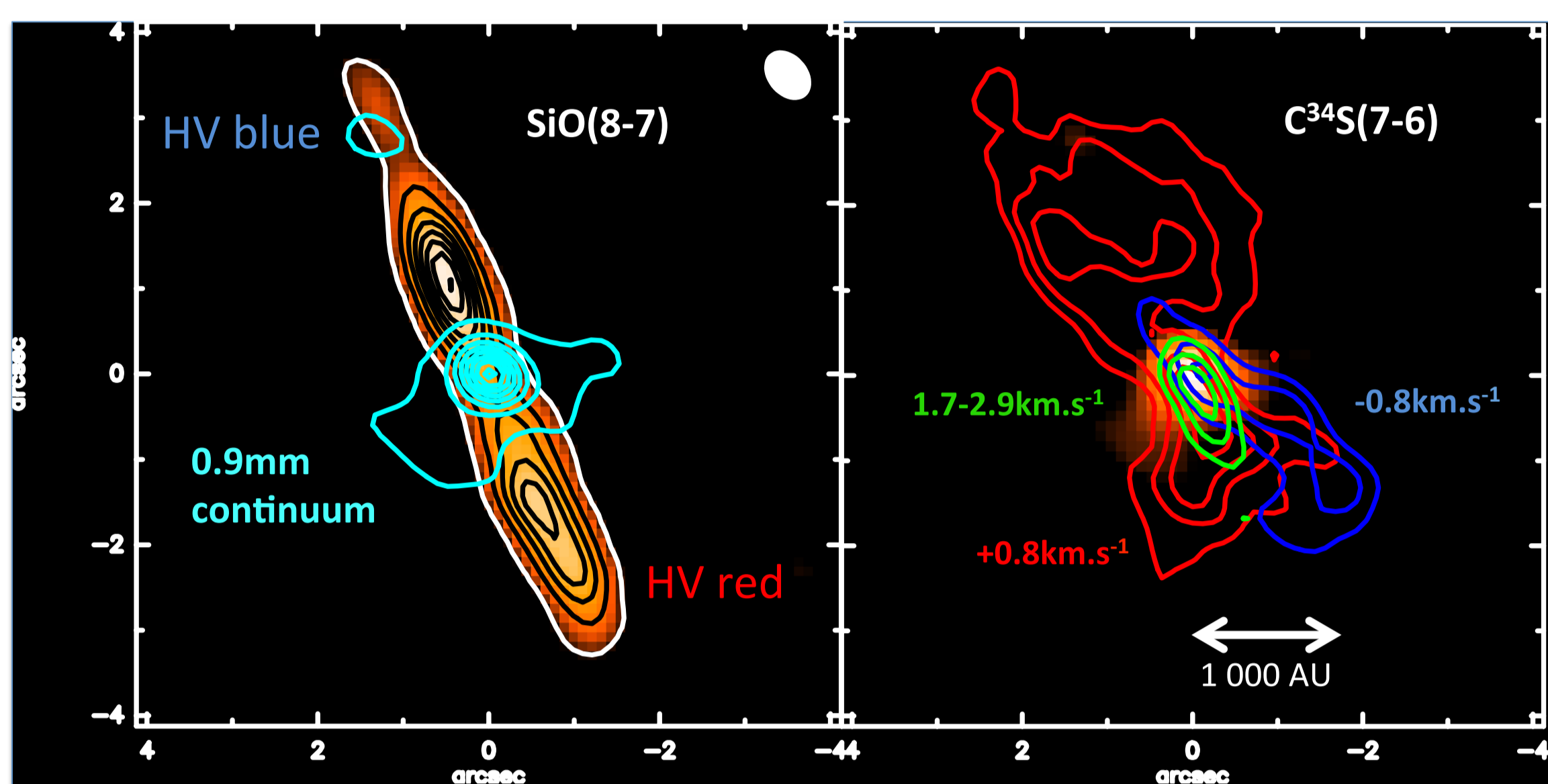
Benoît Tabone¹ (benoit.tabone@obspm.fr), S. Cabrit^{1,3}, G. Pineau des Forêts^{2,1}, J. Ferreira³, C. Codella⁴, F. Gueth⁵

1: LERMA, Observatoire de Paris, PSL Research University, Paris, France 2: IAS, Université Paris-Sud, Orsay, France, 3: IPAG, Université Grenoble Alpes, Grenoble, France, 4: INAF-Arcetri, Firenze, Italy, 5: IRAM, Grenoble, France

Abstract

We show that $C^{34}S$ (7-6) emission from the HH212 protostellar system observed with ALMA exhibits characteristics suggestive of a magneto-centrifugal molecular disk wind extracting mass and angular momentum from disk radii between ~ 0.3 AU and ~ 25 AU, whereas SiO appears to trace a faster collimated jet coming from more internal regions. Moreover, we show that the kinematics of the surrounding outflow cavity at altitudes < 500 AU are consistent with rotating free-falling envelope material.

1 - Context: the ALMA view of HH212



The class 0 source HH212 is one of the best laboratories for studying the interplay of accretion and ejection during the first stages of star formation: Cycle 0 ALMA observations have revealed all the crucial ingredients known to be involved in a protostellar system: a jet, an infalling envelope and a disk possibly in Keplerian rotation (Codella et al. 2014, Lee et al. 2014, Podio et al. 2015), see Fig. 1, left. The $C^{34}S$ (7-6) transition enables us to investigate the accretion-ejection connection through an "intermediate velocity" molecular wind that could be ejected from the disk; and the formation of the accretion disk through a rotating cavity that reveals the kinematics of the infalling envelope (see Fig. 1, right).

Fig. 1 ALMA cycle 0 observations in band 7 (345 GHz) with a synthesised beam of $0.65'' \times 0.47''$ ($290 \text{ AU} \times 210 \text{ AU}$). **Left:** high-velocity bipolar jet seen in SiO(8-7) surrounded by the dusty envelope. **Right:** $C^{34}S$ (7-6) tracing an intermediate-velocity axial wind (green) and a low-velocity rotating cavity (blue and red).

2 – $C^{34}S$ vs SiO: a multi-component outflow

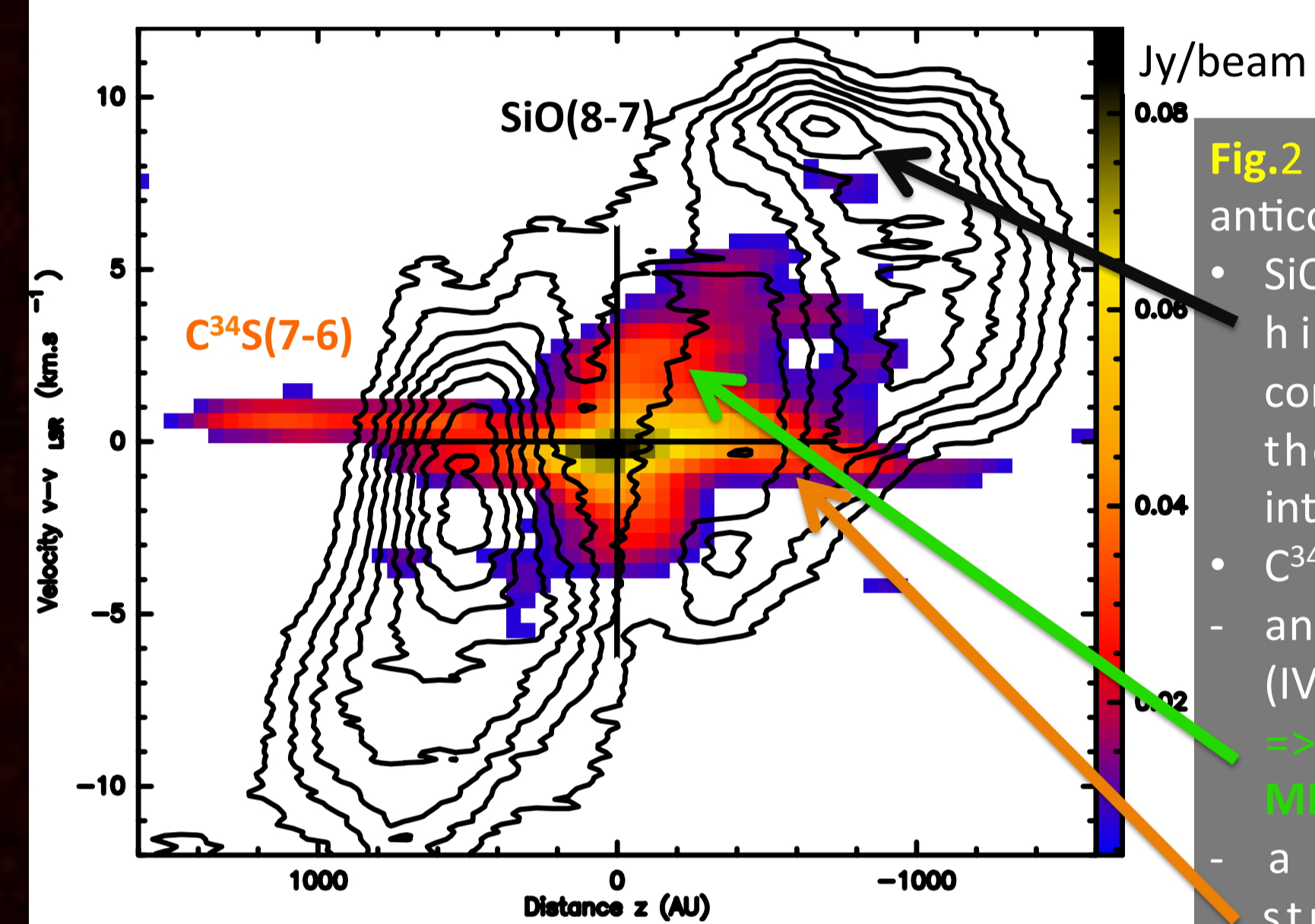


Fig. 2 shows that $C^{34}S$ seems anticorrelated with SiO.

- SiO traces mainly a broad high velocity (HV) component associated with the fast axial jet and internal bowshocks
- $C^{34}S$ exhibits:
 - an intermediate velocity (IV) accelerating flow \Rightarrow extended molecular MHD disk wind?
 - a low velocity (LV) structure at $\pm 1 \text{ km.s}^{-1}$ associated with the cavity

Fig. 2 Position-velocity diagram along the HH212 jet axis of $C^{34}S$ (color-scale) compared with SiO (overplotted black contours from Codella et al. 2014).

3 - MHD disk wind model

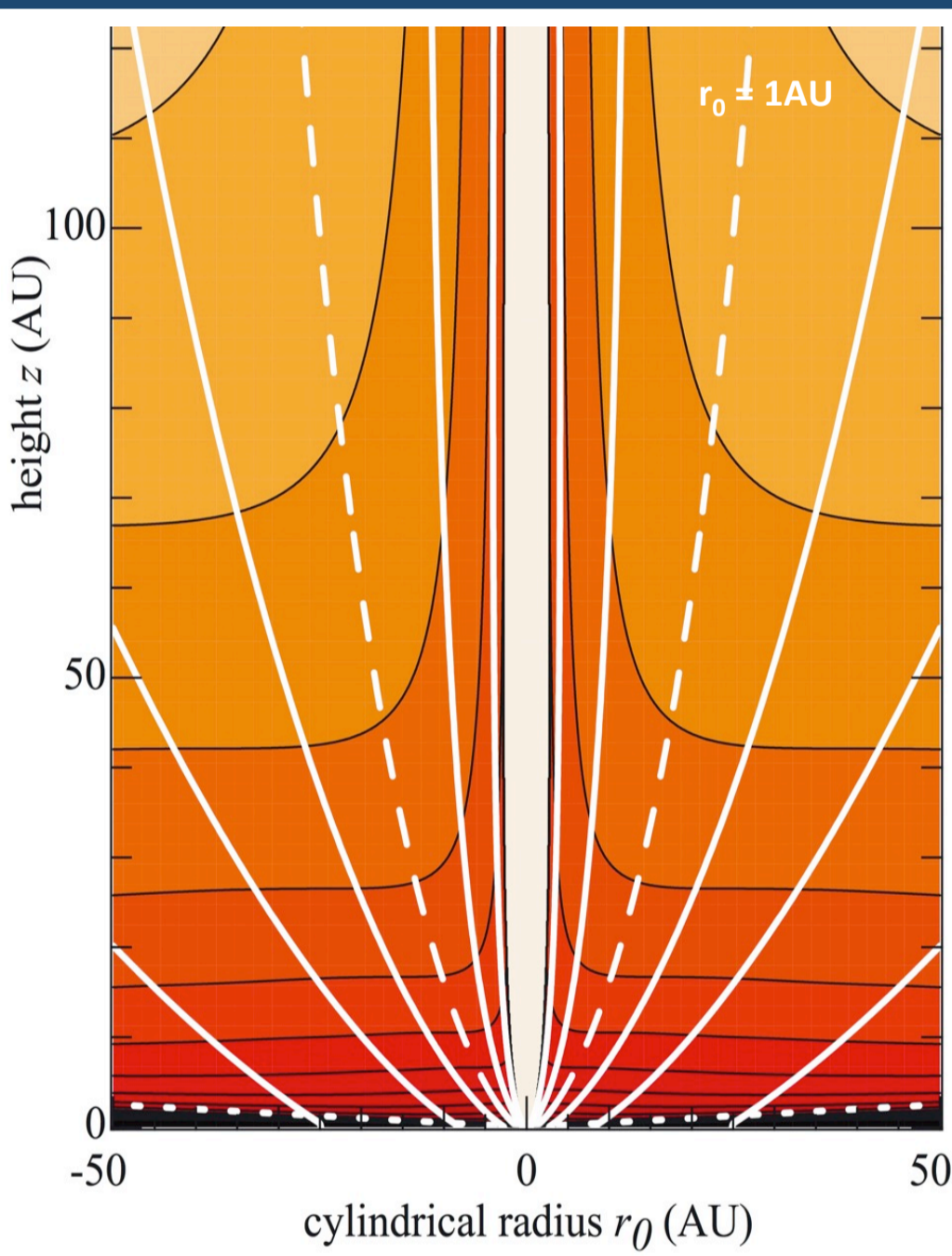


Fig. 3 Density structure of the adopted MHD disk wind model (color scale) from Casse & Ferreira (2000). Streamlines are overplotted in white.

Fig. 3 : MHD disk wind solution (Casse & Ferreira 2000):

- self-similar, axisymmetric, stationary disk wind magneto-centrifugally launched from resistive accretion disk
- extracts all angular momentum flux required for accretion
- magnetic lever arm parameter $\lambda = (r_a/r_0)^2 = 13.8$ matching jet rotation in DG Tau (Pesenti et al. 2004).

Thermochemistry on dusty streamlines (Panoglou et al. 2012 + Yvart et al. 2015):

- chemical network: 129 species, ≈ 1000 chemical reactions
- non-LTE radiative cooling by H_2 , CO, H_2O lines, atomic lines, adiabatic cooling.
- heating by ion-neutral drift, gas-dust coupling.

Non-LTE excitation of $C^{34}S$ under LVG approximation (Tabone et al. in prep).

4 - $C^{34}S > 1 \text{ km.s}^{-1}$: an extended molecular MHD disk wind?

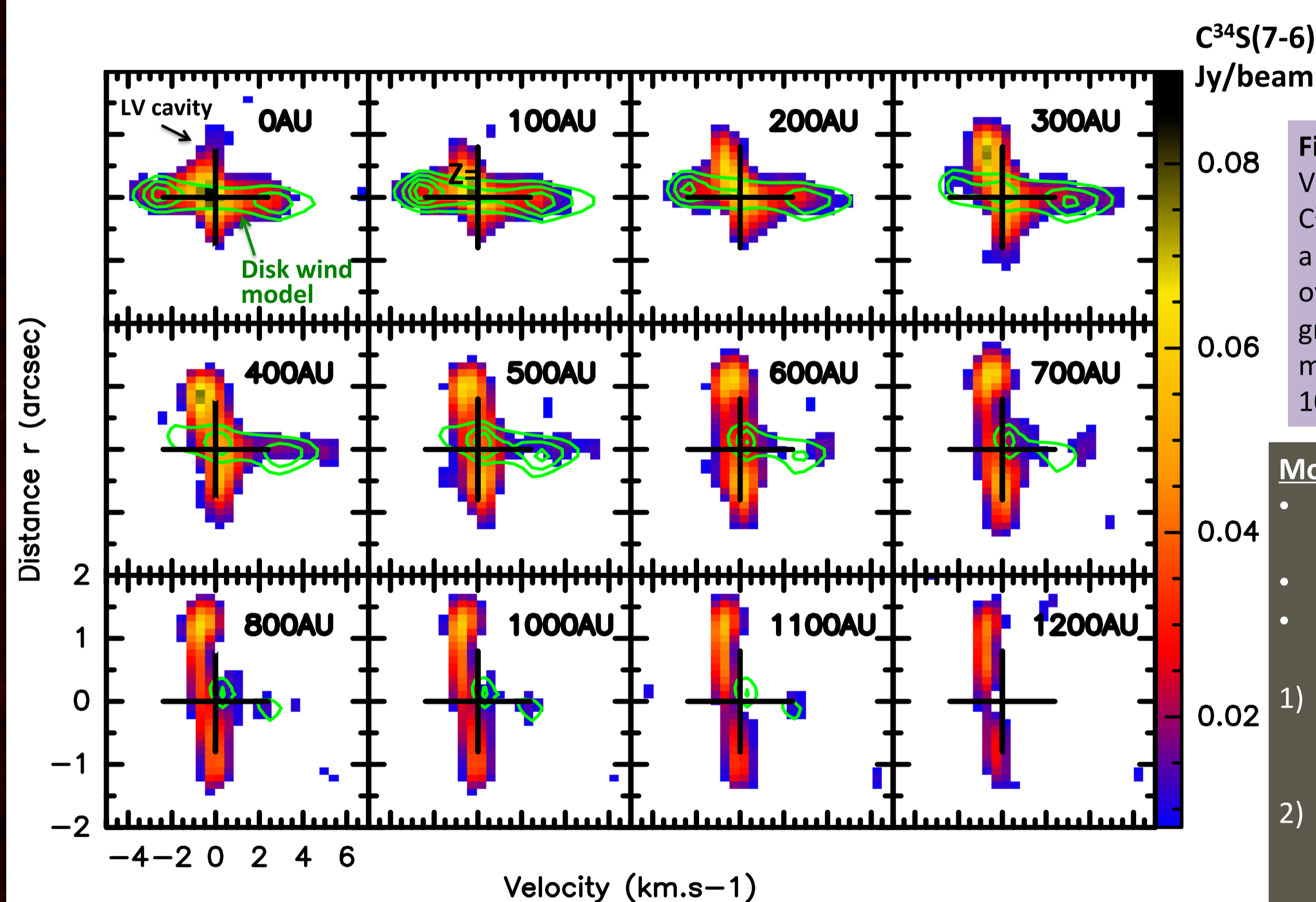


Fig. 4 Observed transverse Position-Velocity cuts across the jet in $C^{34}S(7-6)$ (color scale) at different altitudes z_{cut} (labelled in black) overlaid with synthetic predictions for the MHD disk wind model of Fig. 3 (first contour and steps 10 mJy.beam^{-1})

Model parameters:

- typical class 0 parameters
- $\dot{M}_{\text{acc}} = 5 \cdot 10^{-6} M_{\odot} \cdot \text{yr}^{-1}$, $M_{\star} = 0.1 M_{\odot}$
- launch radius $r_0 = 0.3 - 25 \text{ AU}$
- CS abundance from line intensities:
 - 1) factor 300 enhancement with respect to cold core values (Tafalla et al. 2004)
 - 2) factor 4 enhancement with distance to reach $x(\text{CS}) \approx 10^{-6}$ at 500 AU

5 – Origin of the rotating $C^{34}S$ and $C^{17}O$ cavities

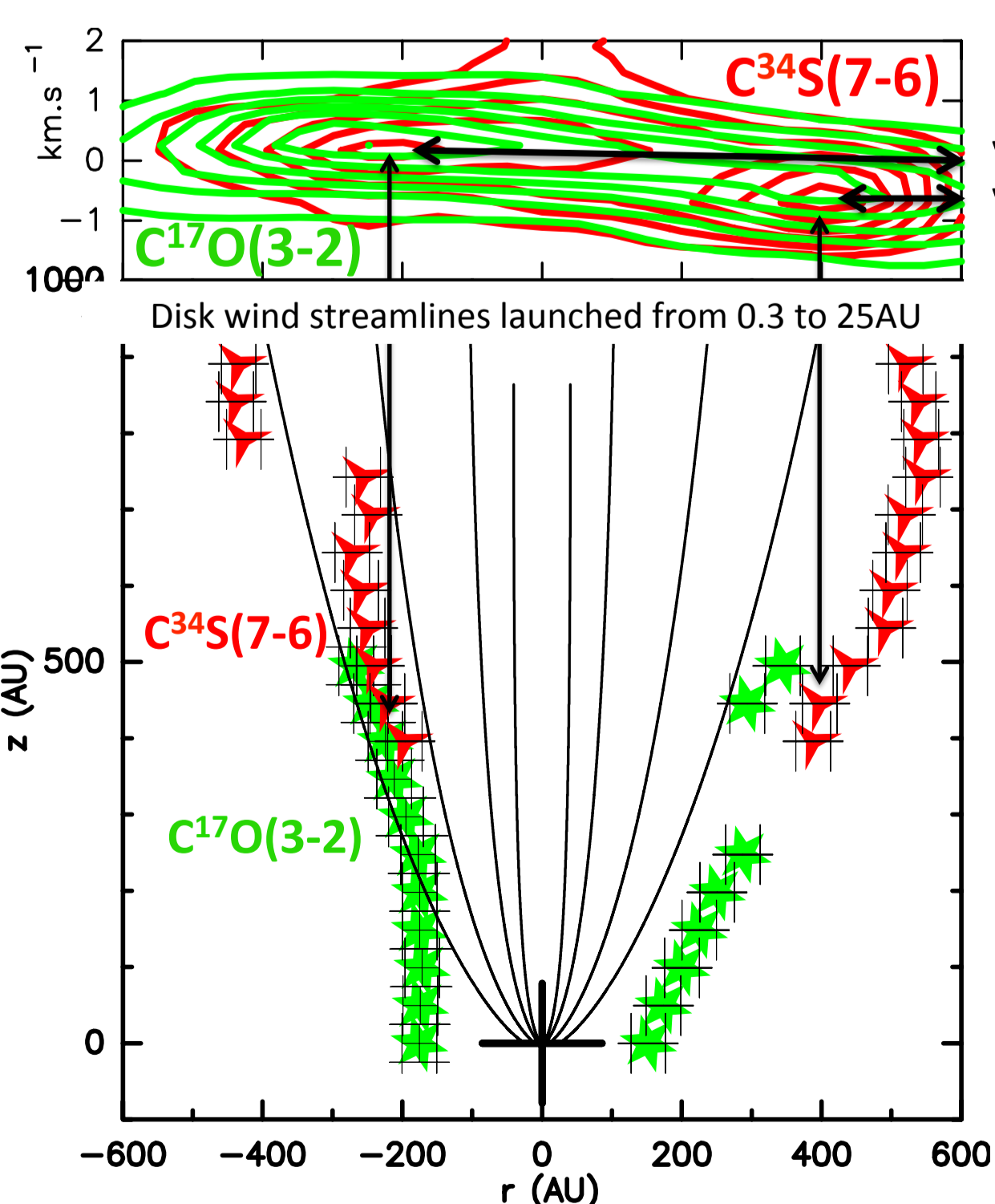


Fig. 5: Cavity morphology and kinematics:

- cavity walls seem to follow the 25 AU disk wind streamline.
- rotation signature: $V_{\phi} = (v_1 - v_2)/2$
- average velocity: $V_z \cos(i) = (v_1 + v_2)/2$

Fig. 6: Comparison with rotating free-fall (Ulrich 1976)

- Good agreement at $z < 500$ AU
- centrifugal radius $r_c = 100-300 \text{ AU} \sim$ disk radius
- deviation from infall above 500 AU: radial expansion induced by disk wind?

Fig. 5 Top: measurement of radius and velocity of each cavity wall using emission peaks in the transverse PV diagrams. Bottom: inferred cavity shape compared with MHD disk wind streamlines launched from radii of 0.3 AU to 25 AU.

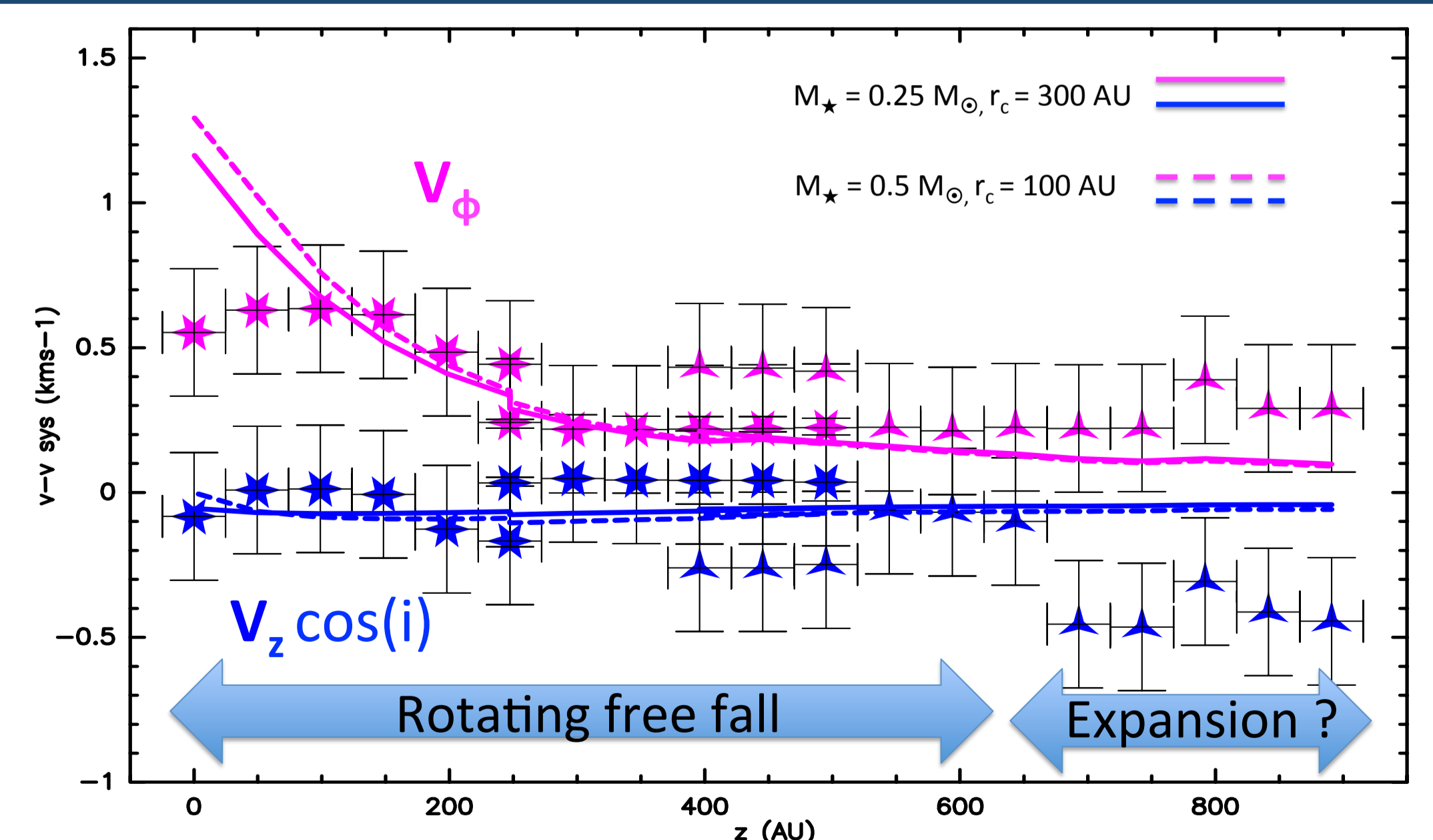


Fig. 6 Measured rotation speed (V_{ϕ}) and projected vertical speed ($V_z \cos(i)$) along the cavity walls compared with the prediction for rotating freefall (Ulrich 1976) with $M_{\star} = 0.25 M_{\odot}$, $r_c = 300 \text{ AU}$ (solid line) and $M_{\star} = 0.5 M_{\odot}$, $r_c = 100 \text{ AU}$ (dashed line)

References

- Cabrit et al. 2012, A&A 548, L2
Codella et al 2014, A&A 568, L5
Lee, C-F et al., 2014, ApJ 786, 114
Panoglou et al., 2012, A&A 538, A2
Pesenti et al. 2004, A&A 416, L9
- Podio et al. 2015, A&A 585, A85
Tafalla et al. 2004, A&A 416, 191
Ulrich, 1976, ApJ 210, 377
Wiseman, 2001, ApJ 550, L97
Yvart et al. 2015, A&A in press